

Bending, buckling, and free vibration analysis of multi-span beams

Aleksandar Nikolić^{1*}

¹University of Kragujevac, Faculty of Mechanical and Civil Engineering, Kraljevo, Serbia

ARTICLE INFO

* **Correspondence:** nikolic.a@mfkv.kg.ac.rs

DOI: 10.5937/engtoday2204019N

UDC: 621(497.11)

ISSN: 2812-9474

Article history: Received 13 December 2022; Accepted 29 December 2022

ABSTRACT

In this paper, the modified segmented rod method (MSRM) will be used for bending, buckling, and free vibration analysis of multi-span beams. Since there is MSRM for a one-span beam in literature, slight corrections will enable the application of this method to the case of multi-span beams. The motivation for this research lies in the fact that there are engineering objects that must be modeled as multi-span beams, such as bridges. The proposed MSRM uses the absolute coordinates of the rigid segments, so the introduction of different boundary conditions as well as the loads can be done easily. The effectiveness of the MSRM was tested through numerical examples where the comparison with current results from the available literature was done.

KEYWORDS

Multi-span beams, Bending, Buckling, Free vibration, Modified segmented rod method

1. INTRODUCTION

Beams as the basic element of many constructions are the subject of research even today. As structural elements in planar models, they are predominantly loaded with axial forces and bending couplings, so it is important to calculate static deformations during bending, critical values of axial forces to prevent buckling, but also to consider the characteristics of the beam during free vibrations. The largest number of studies available in the literature refer to single-span beams. On the other hand, there are continuous systems with repeated beam elements that can be modeled as multi-span beams [1]. Bridges are a typical example of this type of object. The tendency is for bridges to be thinner than before, due to the saving of materials, so they are more sensitive to static and dynamic loads and their analysis in this regard is increasingly important. The literature dealing with this type of beam is plenty. References [2-6] indicate that the topic is still current. In this paper, the modified segmented rod method (MSRM in the further) will be used for the static and dynamic analysis of multi-span beams. This method is developed and described in detail in [7] for the case of a single-span beam with various boundary conditions. Due to the use of absolute coordinates of the endpoints, the results obtained in [7] can be used here with minimal corrections.

2. MSRM MODEL OF THE BEAM WITH ARBITRARY LOADS AND BOUNDARY CONDITIONS

Figure 1(a) shows the MSRM model of the beam with arbitrary loads and boundary conditions which consist of n elementary beam segments of length $\Delta L=L/n$. It was assumed that the beam is generally loaded at points k ($k=1, \dots, n+1$) by the transversal forces F_k and q_k , and force coupling M_k . Note that the force

$$q_k = q\Delta L \frac{p}{p+1}, \tag{1}$$

represents an approximately calculated force that comes from a continuous load, where q is the unit load and p represents the number of elementary beam segments of length ΔL on which the load is distributed.

Each of the elastic segments is further discretized into rigid segments connected by elastic rotational hinges, as shown in Figure 1(b) and explained in detail in reference [7].

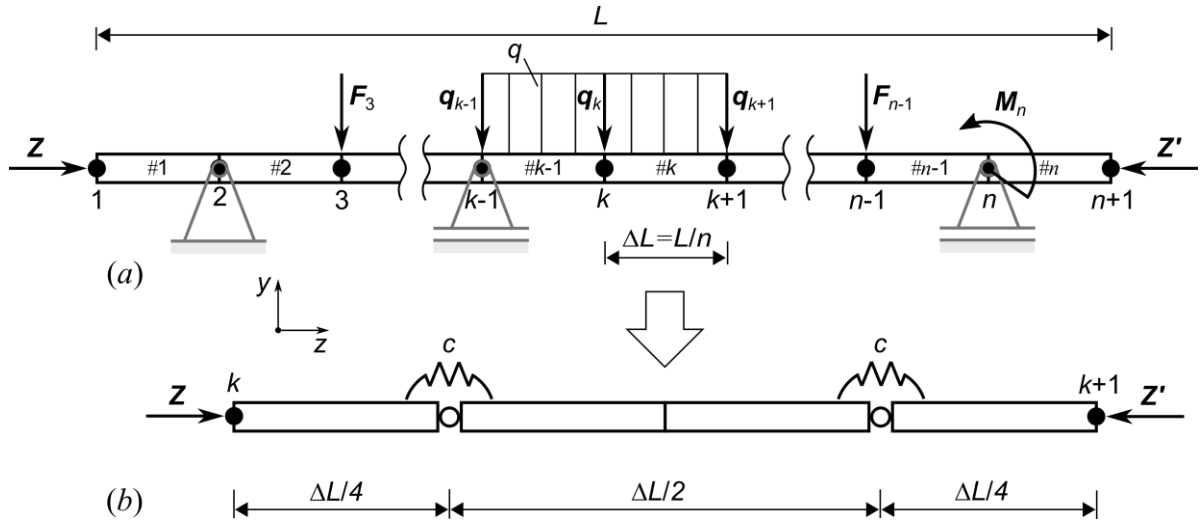


Figure 1: MSRM model [7] of the beam with arbitrary loads and boundary conditions

The differential equations of motion of the considered MSRM model of the free-free beam were given in reference [7]. Relying on them, and taking into account the arbitrary loads that act at the node points $k(q_k, F_k, \text{ and } M_k)$, the differential equations of motion of the considered model have the form:

$$\mathbf{M}\ddot{\mathbf{v}} + (\mathbf{K} - \mathbf{ZS})\mathbf{v} = \mathbf{Q}_v, \tag{2}$$

where

$$\mathbf{X} = \begin{bmatrix} \mathbf{X}_{11,1} & \mathbf{X}_{12,1} & \mathbf{0} & \mathbf{0} & \mathbf{0} & \mathbf{0} & \mathbf{0} \\ \mathbf{X}_{21,1} & \mathbf{X}_{22,1} + \mathbf{X}_{11,2} & \mathbf{X}_{12,2} & \mathbf{0} & \vdots & \vdots & \vdots \\ \mathbf{0} & \vdots & \ddots & \vdots & \mathbf{0} & \vdots & \vdots \\ \vdots & \mathbf{0} & \mathbf{X}_{21,k-1} & \mathbf{X}_{22,k-1} + \mathbf{X}_{11,k} & \mathbf{X}_{12,k} & \mathbf{0} & \vdots \\ \vdots & \vdots & \mathbf{0} & \ddots & \ddots & \vdots & \mathbf{0} \\ \vdots & \vdots & \vdots & \mathbf{X}_{21,n-1} & \mathbf{X}_{21,n-1} & \mathbf{X}_{22,n-1} + \mathbf{X}_{11,n} & \mathbf{X}_{12,n} \\ \mathbf{0} & \mathbf{0} & \mathbf{0} & \mathbf{0} & \mathbf{0} & \mathbf{X}_{21,n} & \mathbf{X}_{22,n} \end{bmatrix} \in R^{2(n+1) \times 2(n+1)}, \tag{3}$$

and $\mathbf{X} = \mathbf{M}, \mathbf{K}, \mathbf{S}$.

The block matrices, which make up the matrices \mathbf{M} , \mathbf{K} , and \mathbf{S} , are given in the explicit form in reference [7] and read:

$$\mathbf{M}_{11,k} = \frac{\rho A \Delta L}{192} \begin{bmatrix} 80 & 14\Delta L \\ 14\Delta L & 3(\Delta L)^2 \end{bmatrix}, \tag{4}$$

$$\mathbf{M}_{12,k} = (\mathbf{M}_{21,k})^T = \frac{\rho A \Delta L}{192} \begin{bmatrix} 16 & -4\Delta L \\ 4\Delta L & -(\Delta L)^2 \end{bmatrix}, \tag{5}$$

$$\mathbf{M}_{22,k} = \frac{\rho A \Delta L}{192} \begin{bmatrix} 80 & -14\Delta L \\ -14\Delta L & 3(\Delta L)^2 \end{bmatrix}, \tag{6}$$

$$\mathbf{K}_{11,k} = \frac{c}{2(\Delta L)^2} \begin{bmatrix} 16 & 8\Delta L \\ 8\Delta L & 5(\Delta L)^2 \end{bmatrix}, \tag{7}$$

$$\mathbf{K}_{12,k} = (\mathbf{K}_{21,k})^T = \frac{c}{2(\Delta L)^2} \begin{bmatrix} -16 & 8\Delta L \\ 8\Delta L & 5(\Delta L)^2 \end{bmatrix}, \quad (8)$$

$$\mathbf{K}_{22,k} = \frac{c}{2(\Delta L)^2} \begin{bmatrix} 16 & -8\Delta L \\ -8\Delta L & 5(\Delta L)^2 \end{bmatrix}, \quad (9)$$

$$\mathbf{S}_{11,k} = \frac{c}{8\Delta L} \begin{bmatrix} 16 & 4\Delta L \\ 4\Delta L & 3(\Delta L)^2 \end{bmatrix}, \quad (10)$$

$$\mathbf{S}_{12,k} = (\mathbf{S}_{21,k})^T = \frac{c}{8\Delta L} \begin{bmatrix} -16 & 4\Delta L \\ -4\Delta L & (\Delta L)^2 \end{bmatrix}, \quad (11)$$

$$\mathbf{S}_{22,k} = \frac{c}{8\Delta L} \begin{bmatrix} 16 & -4\Delta L \\ -4\Delta L & 3(\Delta L)^2 \end{bmatrix}. \quad (12)$$

Vector of coordinates of points $k(k=1, \dots, n+1)$ reads:

$$\mathbf{v} = [\mathbf{v}_1^T \quad \mathbf{v}_2^T \quad \dots \quad \mathbf{v}_k^T \quad \dots \quad \mathbf{v}_n^T \quad \mathbf{v}_{n+1}^T]^T \in \mathbb{R}^{2(n+1) \times 1}, \quad (13)$$

whereas $\mathbf{v}_k = [y_k \quad \varphi_k]^T$ consists of transversal displacement y_k of point k and rotation angle φ_k at this point.

The vector of generalized coordinates corresponding to the previously defined vector \mathbf{v} is of the form:

$$\mathbf{Q}_v = [\mathbf{Q}_{v_1}^T \quad \mathbf{Q}_{v_2}^T \quad \dots \quad \mathbf{Q}_{v_k}^T \quad \dots \quad \mathbf{Q}_{v_n}^T \quad \mathbf{Q}_{v_{n+1}}^T]^T \in \mathbb{R}^{2(n+1) \times 1}, \quad (14)$$

where

$$\mathbf{Q}_{v_k} = [\xi_{F_k} \cdot F_k + \xi_{q_k} \cdot q_k + \xi_{M_k} \cdot M_k]^T, \quad (15)$$

and it holds that each of the coefficients ξ_{F_k} , ξ_{q_k} , or ξ_{M_k} has a value of 1 if a corresponding load is acting at the point k , otherwise it is equal to 0. Since the differential equations of the observed model have been formed for the case of a free-free beam, the introduction of boundary conditions should now be considered. As stated in reference [7], the introduction of different boundary conditions in MSRM is simple. It is only necessary to remove the rows and columns in the matrices \mathbf{M} , \mathbf{K} , and \mathbf{S} , as well as the rows of vector \mathbf{Q}_v , corresponding to the constrained displacements. So, if the beam is pinned at point k then $y_k=0$, or if it is clamped then $y_k=0$ and $\varphi_k=0$.

2.1. Eigenvalue analysis

If we consider free vibrations of the axially loaded beam, then the eigenvalue problem that corresponds to differential equations (2) reads:

$$(\mathbf{K} - \mathbf{ZS} - \omega^2 \mathbf{M})\mathbf{u} = \mathbf{0}_{2(n+1) \times 1}. \quad (16)$$

By solving the characteristic determinant

$$|\mathbf{K} - \mathbf{ZS} - \omega^2 \mathbf{M}| = \mathbf{0}_{2(n+1) \times 1}, \quad (17)$$

the natural frequencies $\omega_r (r=1, \dots, 2(n+1))$ of the considered beam will be determined.

The eigenvector associated with the eigenvalue ω_r , reads:

$$\mathbf{u}_r = [\mathbf{u}_{1,r}^T \quad \mathbf{u}_{2,r}^T \quad \dots \quad \mathbf{u}_{k,r}^T \quad \dots \quad \mathbf{u}_{n,r}^T \quad \mathbf{u}_{n+1,r}^T]^T \in \mathbb{R}^{2(n+1) \times 1}, \quad (18)$$

where

$$\mathbf{u}_{k,r} = [y_{k,r} \quad \varphi_{k,r}]^T. \quad (19)$$

Now, the coordinates of the mode shape points read $\{z_k, y_{k,r}\} (k=1, \dots, n+1)$, where $z_k = (k-1)\Delta L$. By connecting all these points, while respecting the boundary conditions, the approximate r -th mode shape of the beam will be obtained.

2.2. Buckling analysis

Assume now that the beam is loaded only by the axial force Z . When the value of the axial force Z reaches a critical value, the beam will buckle. At that moment, the value of the natural frequency ω of free beam vibration is equal to zero. If we consider that $\omega=0$, the characteristic equation becomes:

$$|\mathbf{K} - Z\mathbf{S}| = \mathbf{0}_{2(n+1) \times 1} \tag{20}$$

By solving this characteristic equation, one can obtain $2(n+1)$ values for Z . The smallest one represents the critical buckling force Z_{cr} . By following the procedure shown for obtaining the mode shapes of free beam vibrations, it is also possible to obtain here the buckling shapes of the beam.

2.3. Bending analysis

Let us now assume that only static loads F_k, q_k , or $M_k (k=1, \dots, n+1)$ act on the beam and that the axial force Z is equal to zero. Also, the assumption is that there are no vibrations under the effect of static loads, so $\omega=0$. If we apply the above assumptions, the differential equation (2) becomes algebraic and takes the form:

$$\mathbf{K} \cdot \mathbf{v} = \mathbf{Q}_v \tag{21}$$

Now, the vector of deformation of the beam reads:

$$\mathbf{v} = \mathbf{K}^{-1} \mathbf{Q}_v \tag{22}$$

Finally, the coordinates of the deflection line of the beam read $\{z_k; y_k\}, (k=1, \dots, n+1)$ where $z_k=(k-1)\Delta L$. By connecting all these points, while respecting the boundary conditions, the approximate shape of the deflection line will be obtained.

3. NUMERICAL EXAMPLES

In the following examples, a beam with a square cross-section of dimensions 0.02×0.02 m will be used, with the following material characteristics: Young's modulus $E=2.1 \times 10^{11}$ Pa and the material density $\rho=7800$ kg/m³. The length of the beam L will be given in each of the examples separately. The results of the finite element method (FEM in the further) will be provided by using the Ansys software. The number of finite elements n will be calculated as the quotient of the total length L of the beam and the smallest dimension of the cross-section (it is 0.02m here) because the beam is modeled as a line body.

3.1. Example 1

Figure 2 shows the four-span pinned-pinned beam. The length of all beam spans is equal whereas the total beam length reads $L=2$ m. The first five dimensionless natural frequencies $(\omega^2 \rho A L^4 / (EI_k))^{1/4}$ are computed by the proposed MSRM and by FEM, with $n=100$ elastic segments used, and compared with the exact results in the closed form obtained in reference [2]. All of these values, including the relative errors between the results of MSRM and FEM to the exact ones placed in parentheses, are shown in Table 1.

The values of the natural frequencies obtained by MSRM are in excellent agreement with the exact values. The largest relative error of 0.023% for the case of the fourth natural frequency proves it. Moreover the first frequency obtained by the MSRM achieves an exact value. The results obtained by the FEM by using the same number of elastic segments n are slightly worse than the results of the MSRM method. So, the largest relative error 0.529% is at the fifth frequency and the smallest 0.125% at the first frequency. Although MSRM has a slight advantage, the results of both methods converge to the exact values quickly enough.

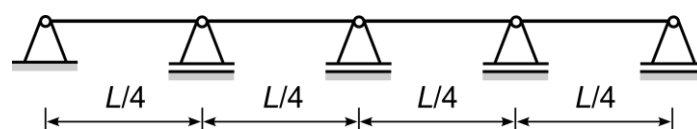


Figure 2: P-P beam with four equally spaced spans

Table 1: The first five dimensionless natural frequencies of P-P beam with four equally spaced spans

Mode number	n=100		Exact [2] (K=10 ¹²)
	MSRM	FEM	
1	12.5664 (0%)	12.5494 (0.135%)	12.5664
2	13.5736 (0.005%)	13.5461 (0.197%)	13.5729
3	15.7085 (0.013%)	15.6568 (0.316%)	15.7064
4	17.8574 (0.023%)	17.7729 (0.450%)	17.8533
5	25.1327 (0.0004%)	24.9999 (0.529%)	25.1328

3.2. Example 2

Figure 3 shows an axially loaded two-span beam at various boundary conditions: (a) clamped-free, (b) pinned-pinned, (c) clamped-pinned, and (d) clamped-clamped. Beam spans are of different lengths, with the first span having a length aL and the second $(1-a)L$, and it holds that $0 < a < 1$.

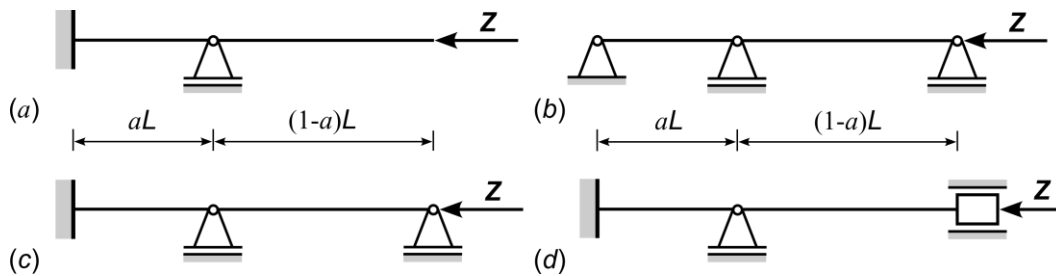


Figure 3: Beam with two spans: (a) C-F, (b) P-P, (c) C-P, (d) C-C.

The exact values of critical buckling force for various parameters under different boundary conditions are obtained in closed form in the reference [6]. By comparing the values of dimensionless critical buckling force $(Z_{cr}L^2/(EI_x))^{1/2}$ obtained by MSRM (with $n=20$ and 40) and the exact ones [6], both shown in Table 2, it is obvious that there is an excellent agreement. The relative errors between these two values which are shown in parenthesis, proven the convergence of the MSRM results to the exact ones as the number of used elastic segments n increase. Moreover, in some situations, using MSRM achieves the exact value, as is the case when $a=0.7$ at C-F and $a=0.1$ and 0.9 at the P-P boundary condition.

Table 2: The critical buckling load Z_{cr} of the beam with two spans at various boundary conditions (BC)

BC	a	MSRM		Exact [6]	BC	a	MSRM		Exact [6]
		n=20	n=40				n=20	n=40	
C-F	0.1	1.7002 (0.124%)	1.6986 (0.029%)	1.6981	C-C	0.1	6.7920 (0.007%)	6.7916 (0.001%)	6.7915
	0.3	2.0267 (0.039%)	2.0261 (0.01%)	2.0259		0.3	8.0247 (0.126%)	8.0323 (0.031%)	8.0348
	0.5	2.5036 (0.02%)	2.5033 (0.008%)	2.5031		0.5	8.9698 (0.189%)	8.9826 (0.047%)	8.9868
	0.7	3.2231 (0%)	3.2231 (0%)	3.2231		0.7	8.0247 (0.126%)	8.0323 (0.031%)	8.0348
	0.9	4.1502 (0.031%)	4.1512 (0.007%)	4.1515		0.9	6.7920 (0.007%)	6.7916 (0.001%)	6.7915
C-P	0.1	4.8640 (0.066%)	4.8616 (0.016%)	4.8608	P-P	0.1	4.8190 (0.004%)	4.8192 (0%)	4.8192
	0.3	5.8248 (0.043%)	5.8267 (0.01%)	5.8273		0.3	5.6314 (0.067%)	5.6342 (0.018%)	5.6352
	0.5	7.1416 (0.113%)	7.1477 (0.028%)	7.1497		0.5	6.2767 (0.103%)	6.2816 (0.025%)	6.2832
	0.7	7.6153 (0.143%)	7.6235 (0.035%)	7.6262		0.7	5.6314 (0.067%)	5.6342 (0.018%)	5.6352

	0.9	6.7242 (0.065%)	6.7275 (0.016%)	6.7286		0.9	4.8190 (0.004%)	4.8192 (0%)	4.8192
--	-----	--------------------	--------------------	--------	--	-----	--------------------	----------------	--------

3.3. Example 3

Figure 4 shows the three-span pinned-pinned beam of total length $L=3\text{m}$, which is loaded by the unit continuous load $q=15\text{ kN/m}$ along the first span, force coupling $M=5\text{ kNm}$ acting in the joint between the second and third span, as well as with the transversal force $F=5\text{ kN}$ acting at the middle of the third span.

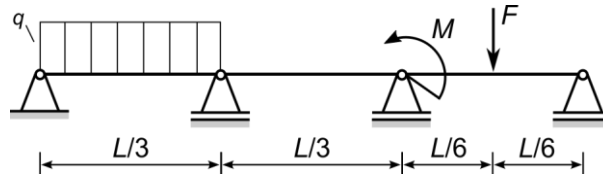


Figure 4: Loaded P-P beam with three spans

The coordinates of the deflection line are obtained in Table 3. The results obtained by using the MSRM and FEM are compared here. Note that $n=150$ elastic segments were used here in both methods. Looking at the relative errors of the MSRM versus FEM results, shown in parentheses, one can see the excellent agreement of the results. A small exception is a displacement at the point $z=1.2\text{ m}$, where a difference of 4.23% is observed. The assumption is that this difference occurs due to the small values of beam deformation at this point. The deflection line of the considered beam obtained by the proposed MSRM is shown in Figure 5.

Table 3: The coordinates of the deflection line of the loaded P-P beam with three spans

z_k [m]	$y_k \times 10^4$ [m]		z_k [m]	$y_k \times 10^4$ [m]	
	MSRM	FEM		MSRM	FEM
0.2	-235.968 (0.87 %)	-238.04	1.6	-245.043 (0.23 %)	- 244.49
0.4	-352.676 (0.93 %)	-355.97	1.8	-238.594 (0.12 %)	- 238.31
0.6	-308.826 (1.02 %)	-312.02	2.2	231.857 (0.13 %)	231.55
0.8	-148.269 (1.25 %)	-150.14	2.4	239.708 (0.23 %)	239.16
1.2	-12.8985 (4.23 %)	-12.375	2.6	165.85 (0.32%)	165.32
1.4	-132.196 (0.51 %)	-131.53	2.8	84.1399 (0.32 %)	83.868

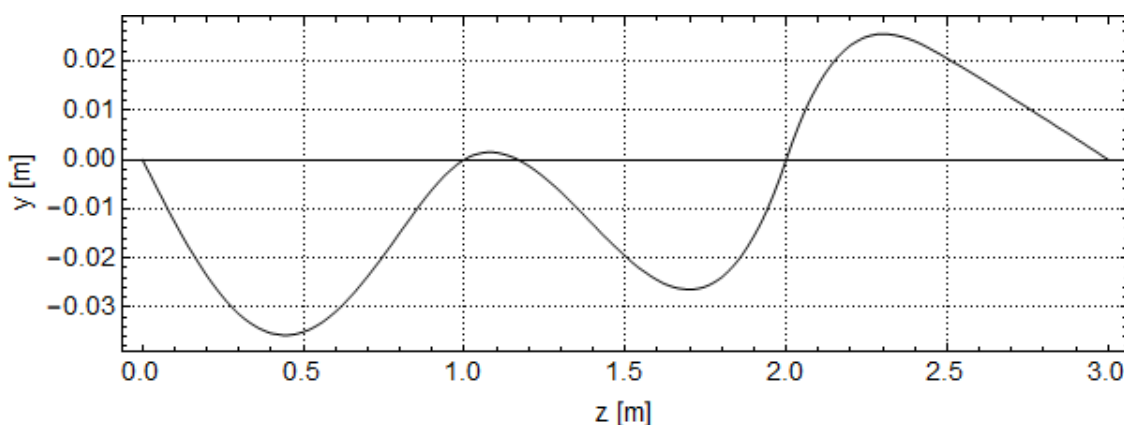


Figure 5: Deflection line of the loaded P-P beam with three spans

4. CONCLUSIONS

It is shown in the paper that the MSRM method developed in reference [7] for the static and dynamic analysis in the case of free-free beams can be easily modified for use in the analysis of multi-span beams. The use of absolute coordinates of rigid segments enables the easy introduction of different boundary conditions and static point loads into the analysis. The efficiency of the proposed method is shown through the three numerical examples, in which the

obtained results are compared with those available in the literature. The relative error between these two groups of results is negligibly small and tends to zero with the increase in the number of used elastic segments. The proposed method has the potential for further use in the analysis of different types of beam-like structures composed of Euler-Bernoulli beams, considering its simplicity and achieved accuracy.

ACKNOWLEDGEMENTS

This research was supported by the Ministry of Education, Science and Technological Development of the Republic of Serbia (Grant No. 451-03-68/2022-14/200108). This support is gratefully acknowledged.

REFERENCES

- [1] V. Kolousek, "Dynamics in Engineering Structures", Butterworths, London (England), (1973)
- [2] J. Luo, S. Zhu and W. Zhai, "Exact Closed-Form Solution for Free Vibration of Euler-Bernoulli and Timoshenko Beams with Intermediate Elastic Supports", *Int. J. Mech. Sci.*, Vol. 213, pp. 106842, <https://doi.org/10.1016/j.ijmecsci.2021.106842>, (2022)
- [3] G. Š. Rončević, B. Rončević, A. Skoblar and R. Žigulić, "Closed Form Solutions for Frequency Equation and Mode Shapes of Elastically Supported Euler-Bernoulli Beams", *J. Sound. Vib.*, Vol. 457, pp. 118-138, <https://doi.org/10.1016/j.jsv.2019.04.036>, (2019)
- [4] Z. Zhao, S. Wen, F. Li and C. Zhang, "Free Vibration Analysis of Multi-Span Timoshenko Beams using the Assumed Mode Method", *Arch. Appl. Mech.*, Vol. 88, pp. 1213-1228, <https://doi.org/10.1007/s00419-018-1368-8>, (2018)
- [5] Y. Xu and D. Zhou, "Elasticity Solution of Multi-Span Beams with Variable thickness Under Static Loads", *Appl. Math. Model.*, Vol. 33(7), pp. 2951–2966, <https://doi.org/10.1016/j.apm.2008.10.027>, (2009)
- [6] C. M. Wang, C. Y. Wang, J. N. Reddy, "Exact Solutions for Buckling of Structural Members", CRC Press, (2005)
- [7] A. Nikolić, "Free Vibration and Buckling Characteristics of Uniform Beam: A Modified Segmented Rod Method", *Int. J. Struct. Stab. Dy.*, <https://doi.org/10.1142/S0219455423500293>, (2022)